Microelectronics Reliability 88–90 (2018) 255–261

Contents lists available at ScienceDirect

Microelectronics Reliability

journal homepage: www.elsevier.com/locate/microrel

Understanding spatial resolution of laser voltage imaging

V.K. Ravikumar[a,b,*], G. Lim[b,c], J.M. Chin[b], K.L. Pey[a], J.K.W. Yang[a]

[a] Singapore University of Technology and Design, Singapore
[b] Advanced Micro Devices Singapore Pte Ltd, Singapore
[c] Nanyang Technological University, Singapore

ARTICLE INFO

Keywords:
Laser voltage imaging
Electro-optic probing
Electrical fault isolation
Fault isolation on FINFETs

ABSTRACT

Laser voltage imaging (LVI) is a commonly used electrical fault isolation technique that is extremely useful in the localization of defects in serial chains and circuits generating specific frequencies within modern integrated circuits. The signals are generated by electro-optic phenomena and the resolution of the tool is therefore constrained by the optical diffraction limit. As such, conventional methods of understanding optical resolution in optical systems such as Rayleigh and Sparrow criteria are currently used to describe the effective resolution. This work formalizes the description of resolution in LVI considering the point spread function of the laser and the electrical circuitry the laser interacts with. Finally, the model is compared with real results across multiple laser wavelengths and is shown to be useful for resolution prediction, determination of optimum probe placement position and predicting the shape of LVI under constrained space conditions.

1. Introduction

Laser voltage imaging (LVI), also known as frequency mapping (FM) or electro-optic frequency mapping (EOFM), is a commonly used electrical fault isolation technique that is extremely useful in localization of defects in serial chains and in circuits generating specific frequencies within modern integrated circuits [1–3]. The underlying principle behind the technique is electro-optic modulation of reflected light, due to interactions between the incident light and components of electrically active elements in integrated circuits such as the source/drain and gate regions of transistors. The modulation, has been shown to specifically occur due to changes in refractive indices within these regions affected by localized electric fields, as well as due to changes in the density of free-carriers which are modulated by changes to the electric state of the device [2].

Being an optical technique, the spatial resolution of LVI is subject to the fundamental limitations of an optical system. As such, conventional methods of understanding spatial resolution in optical systems (without any other physical phenomena) such as Rayleigh and Sparrow criteria are currently used to describe the effective resolution of these systems [4–6]. However, the resolution as dictated by these criteria are not always obeyed by LVI (an electro-optic system) primarily because these criteria do not include the influence of the electrical phase within the devices. With the freedom to influence the electrical phase of the device, LVI can show resolution greater than the conventional criteria. For example, two neighbouring devices such as NMOS and PMOS transistors of an inverter will toggle at exactly opposite phases. That is, when the PMOS switches ON, the NMOS switches OFF and this is in accordance to the construct of a CMOS device. In addition, when two cascading inverters are placed side-by-side to make a buffer as shown in Fig. 1, each of two adjacent transistors have opposite phases. Such competing phases between adjacent transistors can result in a net increase of the spatial resolution of LVI.

This work attempts to formalize the description of spatial resolution of LVI, considering the point spread function of the laser and applying linear superposition algorithms on the modulated reflected light. The electrical state and the physical dimensions (the lateral axes), including the proximity to neighbouring toggling transistors are considered. However, interactions in the axial axis such as the reflection from metal layers and scattering due to the shape of the finFET is not considered. The model is then compared with real results across multiple laser wavelengths, on devices built on sub-20 nm finFET technology. Finally, some applications that use the model for the benefit of LVI and probing are discussed.

2. Spatial resolution

The Rayleigh criterion [7] is defined as the minimum distance between two-point sources that is resolvable through an optical system.

* Corresponding author at: Singapore University of Technology and Design, Singapore.
E-mail address: Venkat-krishnan.ravikumar@amd.com (V.K. Ravikumar).

https://doi.org/10.1016/j.microrel.2018.07.051
Received 27 May 2018; Received in revised form 16 June 2018; Accepted 5 July 2018

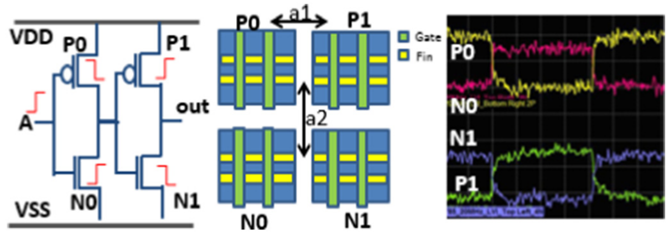

Fig. 1. Layout and schematic of an inverter LVP waveforms show that the phase of the signal on each adjacent transistor (P0, N0), (P0, P1), (N0, N1), (P1, N1) is opposite of each other.

$$R_{(Rayleigh)} = 0.61\frac{\lambda}{NA} \tag{1}$$

$$R_{(Sparrow)} = 0.51\frac{\lambda}{NA} \tag{2}$$

$$R_{(Fourier/Abbe)} = 0.5\frac{\lambda}{NA} \tag{3}$$

Eq. (1) shows the spatial resolution (R) as per Rayleigh criteria where λ is the wavelength of light emitted and NA is the numerical aperture of the optical lens. The Sparrow criterion as described in Eq. (2) is smaller as it is the maximum distance between two-point sources that make it appear as a single source. Conversely, the spatial resolution can be evaluated using Fourier optics [8]. Here, an object under inspection is broken down into spatial frequency constituents. This is analogous to treating the object as a linear superposition of gratings of multiple different spatial frequencies. The objective lens should collect at least 1 diffraction order (0, +1, −1) to resolve the grating of a specific period "***p***" (***p*** = 1/spatial frequency) and as shown in Fig. 2.

The objective is unable to collect the first order from periods that are smaller than the resolution, implying large spatial frequencies (***p*** < ***R***, the resolution) are unable to be collected which leads to blurring of the image compared to the object. The minimum period size for wide angle illumination is shown in Eq. (4) which also coincides with the Abbe's resolution criteria [5].

$$p_{min} = 0.5\frac{\lambda}{NA} \tag{4}$$

We have chosen to use the resolution as formulated by Fourier optics, as it offers a more intuitive understanding of spatial resolution when imaging through a lens system. However, when simulating the laser probe that interacts with the device, it is helpful to visualize and use the Airy disk and to relate its intensity profile as a simple Gaussian distribution. In addition, modern laser scanning microscope uses confocal microscopy that increases the resolution by pin-hole detection to reduce the influence of side-lobes of the imaging beam. The effect on the Airy disk is a sharpening of airy disk profile by 1.4 [9] and Eqs. (5) and (6) estimate the diameter ($D_{AiryConfocal}$) of the Airy disk under a confocal microscope.

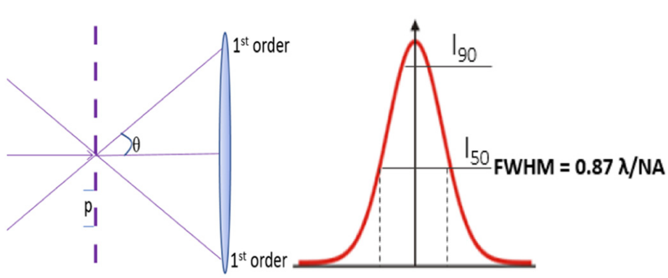

Fig. 2. Spatial resolution can be understood as being able to collect at least 1 diffraction order from a sinusoidal grating with spatial period **p**. The NA of the lens and the wavelength determine the numerical value of **p**. Conversely, the laser probe can be pictured as a Gaussian distribution as on the right as well.

$$D_{Airy} = 1.22\frac{\lambda}{NA} \tag{5}$$

$$D_{AiryConfocal} = \frac{D_{Airy}}{1.4} = 0.87\frac{\lambda}{NA} \tag{6}$$

3. Calculations

A 3-step process is followed in simulating LVI by, first, estimating the laser spread function; second, predicting the modulation capacity of each physical device; and third, convoluting the laser spread function with the modulation capacity, a function that is analogous to raster-scanning the laser across the device.

3.1. Laser point spread function

The optic probe used is assumed to be circularly polarized laser beam focussed to a point and fit a Gaussian profile as described by Fig. 2. The normalized density of distribution (*f*) is provided by Eq. (4), where σ is the standard deviation and completely describes the function [7]. The actual intensity profile of the laser will be the laser power multiplied with the density of distribution.

$$f = \frac{1}{\sqrt{2\pi\sigma^2}}e^{\frac{-(x)^2}{2\sigma^2}} \tag{7}$$

Since, by definition, the full width at half maximum of the intensity (FWHM) is the diameter of the Airy disk, the σ_{FWHM} can be calculated from Eq. (7) by taking the ratio of maximum intensity (x = 0) and half maximum intensity (2x = $D_{AiryConfocal}$) and solving for σ.

$$\sigma = \frac{1}{2\sqrt{2\ln(2)}}D_{AiryConfocal} \tag{8}$$

From Eqs. (6) and (8).

$$\sigma = 0.37\frac{\lambda}{NA} \tag{9}$$

In Eq. (9), we have reduced the σ of the Gaussian distribution into available tool specifications, λ and NA with which we are able to simulate the probe profile conveniently. On the other hand, there are some assumptions in this model of the optic probe. We have ignored the nature of interaction between materials and the incident laser. For example, absorption, scattering, back-reflections, thermal as well as plasmonic interactions within the device are largely ignored. We are also ignoring the axial interaction with the device, as we have simplistically considered the probe as a 2-dimensional point spread function and the device as a 2-dimensional polygon. Finally, we have not considered vectorial description [10] of the laser spread despite operating in the high NA regime. These assumptions, however, have not significantly affected the results (Fig. 4) and qualitative inferences (such as in Section 4 - discussion) could still be made.

3.2. Polygon layout

The physical circuitry simulated is a buffer made up of 4 transistors, 2 PMOS (P0 and P1) and 2NMOS (N0 and N1) from the 14 nm FinFET technology and shown in Fig. 1. Each transistor is of the same size, comprising 2 fins and 2 gates, or 4 transistor nodes. The space between each transistor is defined by the technology specifications. The space between 2 PMOS transistors (or 2 NMOS transistors) is a multiple of the gate pitch (also known as the contacted poly pitch (CPP)). The space between NMOS and PMOS transistors is a multiple of the fin pitch.

The transistors layout is imported into a 2-dimensional matrix "D" in MATLAB. A physical area of 1000 nm × 1000 nm is considered. The laser point spread function is defined into matrix "L".